THE JOURNAL OF PHYSICAL CHEMISTRY B

Article

pubs.acs.org/JPCB

A QM/MM Study of the Absorption Spectrum of Harmane in Water Solution and Interacting with DNA: The Crucial Role of Dynamic Effects

Thibaud Etienne,[†,‡,§] Thibaut Very,[†,‡] Eric A. Perpète,[§] Antonio Monari,*[,†,‡] and Xavier Assfeld[†,‡]

[†]Université de Lorraine - Nancy, Théorie-Modélisation-Simulation, SRSMC, Boulevard des Aiguillettes, BP 70239, 54506, Vandoeuvre-lès-Nancy

[‡]CNRS, Théorie-Modélisation-Simulation, SRSMC, Boulevard des Aiguillettes, BP 70239, 54506, Vandoeuvre-lès-Nancy

[§]Unité de Chimie Théorique et Structurale, Université de Namur, Rue de Bruxelles 61, B-5000 Namur, Belgium

ABSTRACT: We present a time-dependent density functional theory computation of the absorption spectra of one β-carboline system: the harmane molecule in its neutral and cationic forms. The spectra are computed in aqueous solution. The interaction of cationic harmane with DNA is also studied. In particular, the use of hybrid quantum mechanics/molecular mechanics methods is discussed, together with its coupling to a molecular dynamics strategy to take into account dynamic effects of the environment and the vibrational degrees of freedom of the chromophore. Different levels of treatment of the environment are addressed starting from purely mechanical embedding to electrostatic and polarizable embedding. We show that a static description of the spectrum based on equilibrium geometry only is unable to give a correct agreement with experimental results, and dynamic effects need to be taken into account. The presence of two stable noncovalent interaction modes between harmane and DNA is also presented, as well as the associated absorption spectrum of harmane cation.

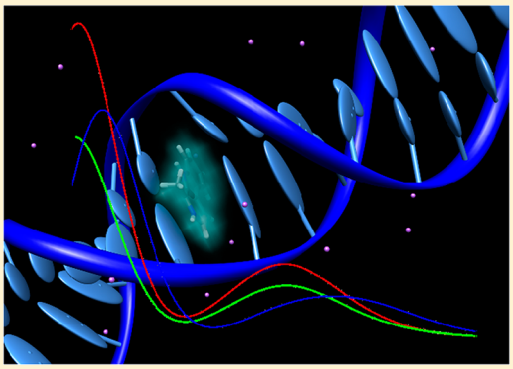

INTRODUCTION

The interaction of small molecules with biological macromolecules and in particular with DNA is nowadays a very attractive and interesting area of research,[1−5] with applications that can cover wide and diverse fields. Indeed, some of the most important applications can be seen in the domain of DNA probes,[6] medical imagery,[7] or modern therapeutic agent developments.[8] The interactions with DNA can lead to irreversible lesions of the macromolecule that can lead to the suppression of the capacity of duplications, an occurrence that can ultimately induce apoptosis and cellular death. Of course such an occurrence can be of extreme importance in cancer therapy,[9−11] evidenced, for instance, by the use of cis-platin drugs,[12−15] where the formation of DNA lesions to kill cancerous cells is a desired feature. Moreover, the quest for compounds able to selectively interact with tumor tissues, and therefore exhibit less side-effects, is extremely active and gives rise to many novel compounds produced and studied.[16]

In addition to covalent linkage, like in the case of cis-platin, the interaction between relatively small molecules and DNA can usually be classified among three main modes.[17−20] The first one is called groove-binding, and it is usually shown by small positively charged molecules; in this case the interactor lies close to the minor or major groove, and the interaction is mainly driven by electrostatic stabilization with the negatively charged DNA backbone. In the second interaction mode, called intercalation, the interacting molecule is able to insert between two base pairs, where it is stabilized by π-stacking interactions. Finally the third case, insertion, is characterized by the substitution of one of the DNA bases by the interacting molecule that takes its place in the double helix structure. Note that the last two interaction modes necessitate the presence of rather extended planar structures to insert into the DNA structure.

Important features exhibited by some xenobiotic molecules in interaction with nucleic acids are related to their peculiar photophysical and photochemical properties, and hence to the nature of their electronic excited states.[13,21] More precisely, the presence of the complex environment constituted by the biological macromolecules is in some cases able to substantially modify the response of the chromophores to light,[22,23] as well as to significantly change the luminescence properties. In that context one could, for instance, think to the well-known light switch effect exhibited by some ruthenium complexes.[1,2,24] Some of the latter do not emit in aqueous solution, but exhibit a very strong luminescence in the presence of DNA. Such a property can be of extreme importance for their use as a DNA probe. Indeed, what is extremely striking is the possibility to

Received: February 20, 2013
Revised: March 28, 2013

   dx.doi.org/10.1021/jp4017882 | J. Phys. Chem. B XXXX, XXX, XXX−XXX

tune the behavior of the light-switch effect by simple and small modification of ligands.[25] For instance, upon substitution of ancillary ligands, the photophysical behavior of the complex is completely reversed, the latter becoming emissive in water, while luminescence is quenched in the presence of DNA.[26] The latter phenomenon can be related to an electron transfer occurring in the excited state, and leading to a DNA base (most often guanine) oxidation.[8,27] This latter characteristic is of seminal importance since the electron transfer from DNA can lead to a cascade of reactions inducing irreversible lesions of the macromolecule, thus the excited state mediated DNA oxidation could be efficiently exploited in phototherapy to selectively induce cellular death only on the tissues exposed to the ultraviolet/visible (UV/vis) light. Apart from the well-known ruthenium complexes, recent studies have shown that iridium or osmium organometallic systems can interact with DNA and induce excited state mediated charge transfer, ultimately provoking an electron current through the DNA.[28]

Moreover, small organic molecules are also known to have strong affinity to DNA, being able to form noncovalent interactions that can lead to toxicity[29] but also therapeutic effects.[30] One can consider, for instance, polychloro-biphenyle systems (also known as dioxine -like molecules[21]) or to the class of β-carboline systems.[31] The latter family of molecules (see Figure 1) is characterized by a planar structure derived

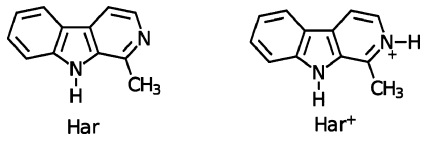

Figure 1. The chemical formulas of neutral Harmane (Har) and Harmane cation (Har^+).

from the presence of three fusioned aromatic rings, a central pyrrole, a phenyl ring, and a pyridine fragment, the substitutent on the pyridine and pyrrole defining the members of the family. β-Carboline interest relies strongly on their important biological activity.[32] Indeed, the former are able to not only interact with DNA but also to interact with many neurotransmettors and neuromodulators;[33−35] these properties have paved the way to their use as efficient antibiotics and antiparassitary agents[36−43] as well as anticancer drugs.[44−51] The other important aspect of this class of compounds is related to their interaction with UV/vis light; indeed β-carbolines absorb in the visible region of the spectrum and can emit through fluorescence.[52] These properties have allowed for their use as photosensitizers against fungi and bacteria,[53] while their capacity to photoactivate the production of singlet oxygen[27] makes them ideal candidates to be used as photodynamic therapy sensitizers.[54,55] In the present contribution we will concentrate on the study of the photophysical properties of harmane (Har) and its cationic form (Har^+) derived from protonation of the pyridine nitrogen atom (Figure 1). Indeed the neutral and protonated forms of the molecule coexist in aqueous solution at physiological pH, while, as recently shown by Paul et al.,[20] the protonated form is able to selectively interact with DNA. In particular, two principal interaction modes are supposed, namely, groove binding through minor groove and intercalation. The intercalation is also favored by the planar structure and by the relatively low steric hindrance.

The computation of absorption spectrum, and in general of excited state properties, in complex systems and media is a task requiring the use and application of well-suited computational methods and balanced protocols.[56,57] In particular, solvatochromic effects induced by the solvent and by the macromolecular media should be carefully taken into account. In the case of homogeneous media (for instance, a chromophore in solution), one popular strategy relies on the use of a polarizable continuum medium (PCM[58]) to take into account the environment. An alternative strategy can consist in the use of hybrid quantum mechanics/molecular mechanics (QM/MM) methods treating the solute quantum mechanically and the solvent molecules using a classical force field.[59−65] Obviously, in order to take into account a meaningful statistical sampling over the different solvent conformations, one should couple this strategy with molecular dynamics (MD) techniques, and consider the final absorption spectrum as a superposition of different spectra obtained from several snapshots. The latter strategy will also allow one to take into account the contribution due to the vibrational degrees of freedom of the chromophore, and hence to recover asymmetry of the spectral bands, as well as the dynamic effects affecting the position of the transition maxima. Moreover, in the case of the interaction with macromolecular and inhomogeneous environments, the use of QM/MM techniques becomes compulsory in order to meaningfully take into account the different effects of the medium.

QM/MM methods are also extremely useful from an analytical point of view since they allow one to separate the environment effects between purely geometric, i.e., environmentally induced geometric distortion, electrostatic effects due to the interaction with the MM point charges, and polarization due to the response of the environment to the redistribution of the electronic density upon the transition.

In the present Article, the absorption spectrum obtained from equilibrium geometry by using PCM and by QM/MM plus MD techniques will be compared in the case of an aqueous solution. The two supposed interaction modes of Har^+ with DNA will be tackled using MD techniques, and the resulting trajectories will be used to extract snapshots to compute absorption spectra for the two cases. Results will be compared with recently published experimental findings.

The present article is organized as follows: computational strategy and details will be given in Section 2, results for water solution will be presented in Section 3, the interaction with DNA will be considered in Section 4, and conclusions will be drawn in Section 5.

■ COMPUTATIONAL STRATEGY AND DETAILS

In order to take care of the effects of the environment, as previously underlined, two different approaches have been considered: in particular, in the case of water-solvated Har and Har^+, the system has been treated at density functional theory (DFT) and time-dependent density functional theory (TDDFT) by using PCM[66,67] to model the environment. The first six excited states have been computed for the neutral and the cationic system. Water dielectric constant has been used, and the cavity has been built basing on van der Waals radii of constituent atoms. The excited state energy and oscillator strengths have been computed from equilibrium geometry as vertical transitions in the framework of the Franck−Condon principle. Optimization and excited state calculations have been performed using the augmented triple-ζ

dx.doi.org/10.1021/jp4017882 | J. Phys. Chem. B XXXX, XXX, XXX−XXX

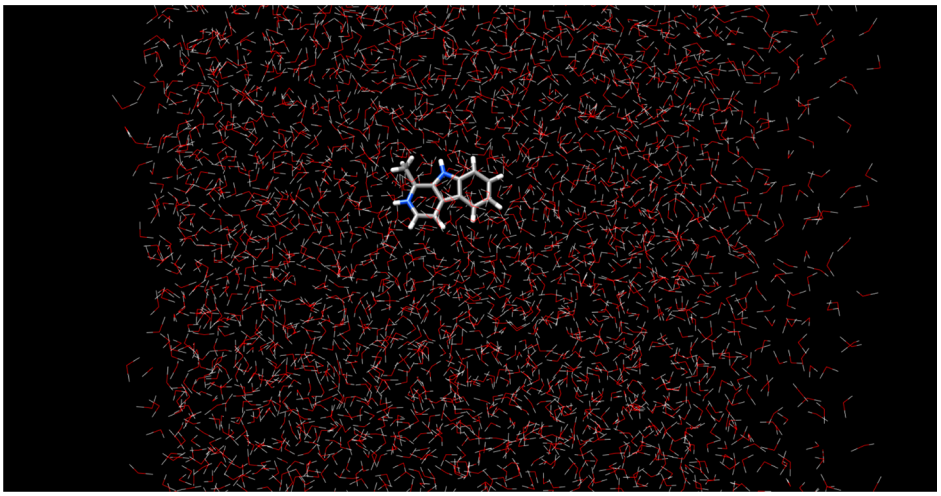

Figure 2. The simulation box for Har^+ in water solution. Water molecules in wire representation the chromophore in sticks.

quality 6-311++G(d,p) basis set,[68] and the PBE0 hybrid functional.[69] Note that tests performed using different functionals, namely, B3LYP[70] and long-range corrected CAM-B3LYP,[71] have shown no significant deviation from PBE0 values. Moreover, some tests performed at the N-electron-valence second order perturbation theory (NEVPT2), has shown a very good agreement with the TDDFT results, the deviations for the visible part of the spectrum being less than 10 nm. Vertical transitions have been convoluted with Gaussian functions of fixed half-length-width of 0.3 eV to partially recover the enlargement of the absorption bands due to vibrational motion and solvent conformations.

Alternatively, the chromophore has been embedded in an explicit cubic box of water molecules of initial size 50 × 50 × 50 Å containing 3181 solvent molecules (Figure 2). Note that in the case of cationic specie, one chlorine anion has been added to ensure electroneutrality. The solvent has been represented using the TIP3P[72] model for water, the solute is represented using generalized amber force field (GAFF[73]), and charges have been obtained by quantum chemistry calculation on the isolated molecule. After an equilibration phase in the isotherm and isobar (NPT) ensemble to reach a temperature of 300 K, a pressure of 1 atm, and the density of liquid water, a 2.0 ns MD trajectory has been run again in the NPT ensemble, using a time step of 1.0 fs. Ninety snapshots have been randomly extracted from the trajectory, and the distance between the snapshots has been chosen to ensure that the autocorrelation between subsequent structures is close to zero, i.e., each snapshot being independent, the ensemble can be considered as statistically significant. Electronic excited states have been computed on each snapshot by using a mixed QM/MM strategy.

In particular, the full Har (Har^+) molecule has been included in the quantum region. In addition to that, since the solute can form labile hydrogen bonds with solvent molecules, for each snapshot we added water molecules to the quantum part when they were at a distance not greater than 2.0 Å from the chromophore. The quantum part has again been treated at the TDDFT level using PBE0 and 6-311++G(d,p) basis. Again the first six excited states have been computed for each snapshot. The final spectrum has been produced by the convolution of all the vertical transition energies of all the snapshots, using Gaussian functions of fixed half-length-width of 0.2 eV. Note that this strategy allows one to take into account the asymmetry of the band shape, and, because of the sampling of conformation space, it is also able to retrieve vibrational effects and solvent conformations that may affect the general shape of the spectrum. The effects of the environment were analyzed by considering pure mechanical embedding (ME) of the chromophore, the electrostatic embedding (EE) thanks to the inclusion of the classical subsystem point charges into the Fock operator, and polarizable embedding (PE) treated via the use of the electronic response of the surrounding (ERS) technique as developed in our laboratory.[56] Note that the latter technique is able to retrieve polarization effects without the use of a polarizable force field,[74] and is based on the embedding of the quantum part in a polarizable continuum, characterized by its dielectric constant extrapolated at infinity frequency. The polarizable continuum interacts with the quantum part, but not with the MM point charges, and it models the response of the environment via a self-consistent reaction field (SCRF) algorithms. Its role is to model the instantaneous reorganization of the electronic density distribution of the environment induced by the change in the electronic density of the chromophore subsequent to the excitation. Note that while reorientation of the environment molecules is excluded in the framework of the Franck−Condon approximation, the polarization, involving only electron redistribution, should be properly accounted for. The previous technique has been proved to be efficient to recover important polarization effects in the determination of absorption spectrum of macromolecular and biological systems.[59,75]

In the case of the interaction with DNA, we have only considered the QM/MM approach, and only the Har^+ cation was studied. In particular, two different initial configurations were generated, one in which the chromophore is intercalated between the DNA base pairs, and the other one in which the cation is interacting with the macromolecule close to the minor groove. The chosen double-strand DNA in B-form was composed of 15 base pairs of sequence 5′-AGGCCTCTGGTCTCC-3′. The previous sequence, representing DNA extracted from calf thymus, is quite commonly used in spectroscopic determination and was used by us in the modeling of interactions between ruthenium complexes and DNA.[1,2] DNA and Har^+ cation were solvated with about 50000 water molecules using a parallelepiped box of initial size 80 ×

dx.doi.org/10.1021/jp4017882 | J. Phys. Chem. B XXXX, XXX, XXX−XXX

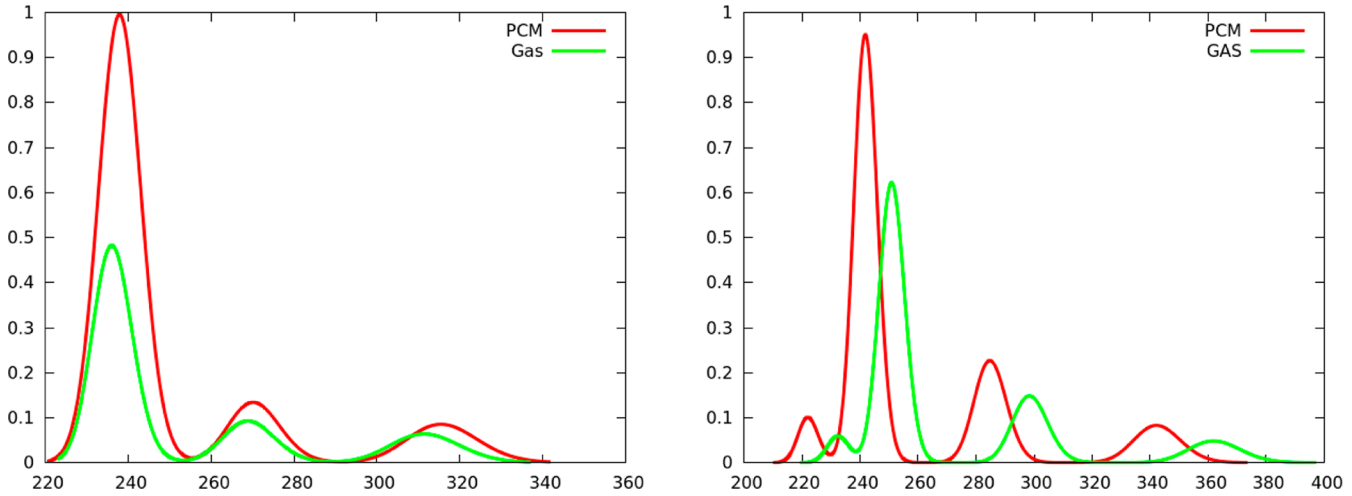

Figure 3. TD-DFT computed spectra of Har (left) and Har^+ (right) in gas phase and with PCM. Wavelengths in nanometers; intensities in arbitrary units.

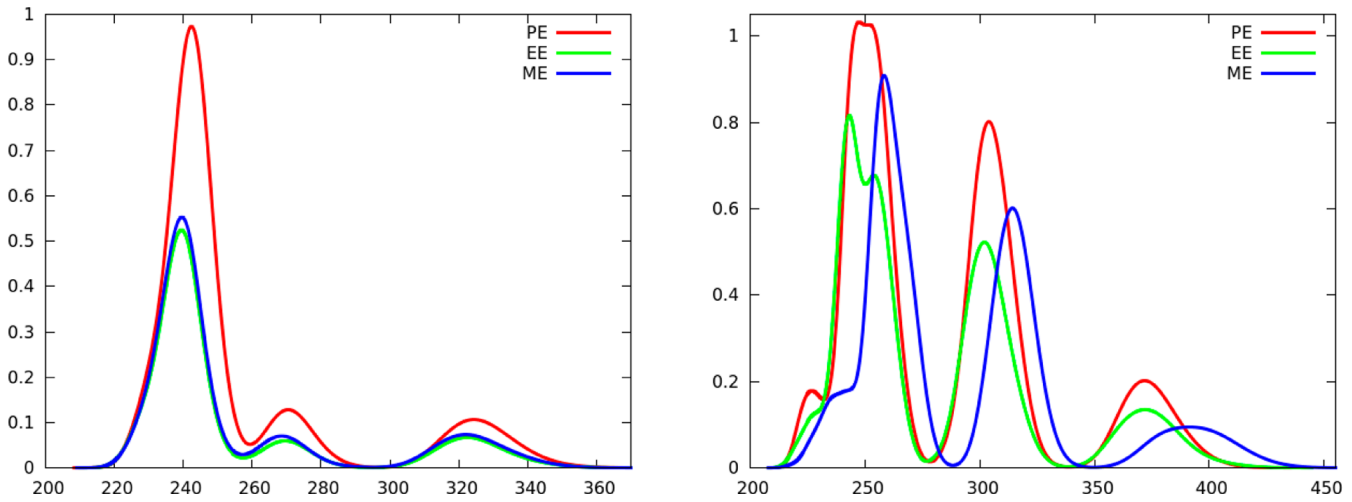

Figure 4. Computed TD-DFT for neutral harmane (right) and cation (left). Spectra are computed as an average over MD snapshots. Wavelengths in nanometers; intensities in arbitrary units.

80 × 100 Å. DNA was modeled using amber99 force field,[76] and 27 sodium ions were added to the box to ensure electroneutrality. Both initial configurations have been equilibrated at 300 K and 1 atm, and a 2.0 ns MD trajectory has been run on each in the NPT ensemble again using a 1.0 fs time step. From both trajectories we extracted 90 snapshots on which TD-DFT was used to compute the excited states at QM/MM level. Note that no DNA base pair was included in the quantum region and that, again, the three different ME, EE and PE embeddings have been taken into account. Coherently with the calculations of aqueous solution, excited states have been computed using PBE0 functional and 6-311++G(d,p) basis, and the lowest six excited states have been considered. Vertical transitions have again been convoluted with Gaussian functions as in the previous case.

All QM and QM/MM calculations have been performed with a local modified version of the Gaussian09 code,[77] coupled with Tinker.[78] NEVPT2[79] calculations have been performed using the Orca code.[80] MD trajectories have been performed using NAMD code.[81]

WATER SOLUTION

The experimental absorption spectrum of aqueous harmane solution at pH 7, as well as the one of other similar β-carbolines,[20] is dominated in the visible region by two relatively intense and large absorption bands: the first appearing at about 340 and the second at about 370 nm. The two bands are assigned to the neutral and the cationic species, respectively. Indeed, the pK_a of the pyridin nitrogen of harmane[20] (7.7) implies that in neutral solutions the protonated and deprotonated systems are present in a roughly 1:1 ratio. In addition to these bands, the neutral harmane spectrum is characterized by two more absorption bands appearing at about 290 and 250 nm,[52] while the cation presents two additional maxima at 300 and 250 nm.[52]

In Figure 3 we report the computed TD-DFT spectra using PCM to account for solvent effects, as well as the spectrum computed in gas phase for Har and Har^+. The spectra are obtained by convoluting vertical transition from the ground state equilibrium geometry. As one can see, both in the case of the neutral specie and the cation, the PCM absorption bands in the visible region are significantly blue-shifted compared to the experiment, with Har giving a maximum at about 320 nm and

dx.doi.org/10.1021/jp4017882 | J. Phys. Chem. B XXXX, XXX, XXX−XXX

Har^+ giving a maximum at 345 nm. The UV bands, on the other hand, are less dramatically affected. We underline here that other exchange-correlation functionals all give similar results, and that the basis set used can be considered as converged. Moreover, the transition responsible for the lowest energy absorption maximum can clearly be expressed as a simple highest occupied molecular orbital to lowest unoccupied molecular orbital (HOMO−LUMO) transition of $\pi-\pi^*$ character for which TD-DFT is known to provide reliable results.[82]

In comparing PCM results with the gas phase spectrum, one can see that in the case of the neutral specie, the two descriptions do not differ significantly, with solvent effects accounting only for a very small red-shift of less than 10 nm. On the other hand, the behavior of the cation specie is much more interesting. Indeed, in the case of the gas phase, the spectrum appears significantly red-shifted with a maximum much closer to the experimental value appearing at about 365 nm. Therefore the inclusion of solvent effects seems to actually deteriorate the quality of the results. Note also that the present blue-shift of the spectrum is not due to particular interactions, like hydrogen bonds, with only few water molecules. Indeed, the explicit inclusion of two water molecules close to the nitrogen atoms and the subsequent full geometry optimization followed by TDDFT calculation do not induce any significant modification of the spectrum and of the absorption maxima. It appears evident that even for relatively simple molecules, such as the present one, good reproduction of the absorption spectrum relies on the subtle and balanced interplay between different effects taking place on the system. In particular, the electrostatic and polarization interactions between the solute and the solvent should be considered together with the coupling between the vibrational degrees of freedom of the chromophore and the solvent conformations. Indeed, such coupling could lead to important dynamic and geometric effects that can ultimately strongly modify the general appearance of the spectrum and the position of the bands.

In Figure 4 we report TD-DFT spectra computed convoluting different snapshots extracted from the MD trajectory of the solvated Har and Har^+. If we consider the highest level of theory, PE, we can easily notice a very good agreement with experimental results. Indeed, in the case of the neutral system, we get first absorption maximum at about 330 nm, while Har^+ gives a maximum at 370 nm. In addition, in the UV part of the spectrum, one can see two additional bands centered at 240 and 270 nm for the neutral specie and at 250 and 300 nm for the cation.

Moreover, it should be noticed that electrostatic and polarization effects induce only a slight modification on the value of the absorption maximum for the Har system, only producing a small red-shift. Again the case of the cation is far more interesting: first of all, as expected since the chromophore is charged, electrostatic effects are this time much more important. ME alone on this system gives a very red-shifted maximum with absorption at about 400 nm, electrostatic effects (EE) shift the maximum toward shorter wavelengths, accounting for about 40 nm, while polarization (PE) slightly shifts the maximum back toward the red. Notice, however, the important effect of PE on the relative intensities. The previous fact is coherent with the observation that gas-phase spectrum from equilibrium geometry was significantly red-shifted compared to the PCM one.

The less strong effects exhibited by the PE can be easily understood when considering that the dipole moment is practically unaltered when going from the ground to the excited state with a deviation of less than 10^{-3} D. In any case, it appears evident that geometric, dynamic, and vibrational effects are crucial to get a precise description of the absorption behavior of such a molecule. Indeed, by analyzing the individual snapshots, one can see that the first transition spans a large energetic domain, with vertical transitions (for the PE case) occurring from 360 to 400 nm, depending on the snapshot and obviously peaking at about 370 nm. This shift can be rationalized considering the important deformation of the planarity of the fusioned ring induced by out of plane vibrations, one can indeed recognize deviation from planarity accounting for 20° or more. As already cited, the first excited state, responsible for the absorption at 370 nm, is dominated by HOMO to LUMO transition (Figure 5), implying a $\pi-\pi^*$ nature. Notice that the

Figure 5. Isodensity surface for the HOMO and LUMO orbitals of Har^+.

HOMO orbital presents a bonding interaction extending on the whole three-ring system, while in the LUMO orbital this interaction is of antibonding character. Therefore, the loss of planarity induces a destabilization of the ground state, reducing the delocalization among the three rings, while the excited state is much less affected. Electrostatic effects can then partially recover the stabilization of the ground state shifting the transition back to higher energy. The fact that the first excited state is essentially of $\pi-\pi^*$ nature, and therefore does not exhibit any significant electronic density spatial reorganization, also explains the fact that the dipole moment is practically the same for the two electronic states.

INTERACTIONS WITH DNA

After having analyzed the behavior of Har and Har^+ in water solution, we tackle the problem of the interaction of Har^+ with DNA. As already said, and following ref 20, two interaction modes have been chosen: groove-binding to the minor groove and intercalation. To assess for the stability of the interaction modes, we run a MD simulation of 2.0 ns on the two different configurations. In Figure 6 we report two representative snapshots obtained during the trajectory; note that we emphasize in green the region of space spanned by the chromophore.

It is evident that the Har^+ forms two stable aggregates with DNA, intercalation and groove-binding being perfectly conserved all along the trajectory. Note also that, as expected, the motion of the intercalated Har^+ is less free than in the case of groove binding; indeed, in the former case, the chromophore has access to a very limited region of space compared to the electrostatical interaction. However, in the case of groove-binding, even if Har^+ is free to explore a much larger region of space, it is confined in close proximity to the groove. The only important collective motion can be considered as diffusion

dx.doi.org/10.1021/jp4017882 | J. Phys. Chem. B XXXX, XXX, XXX−XXX

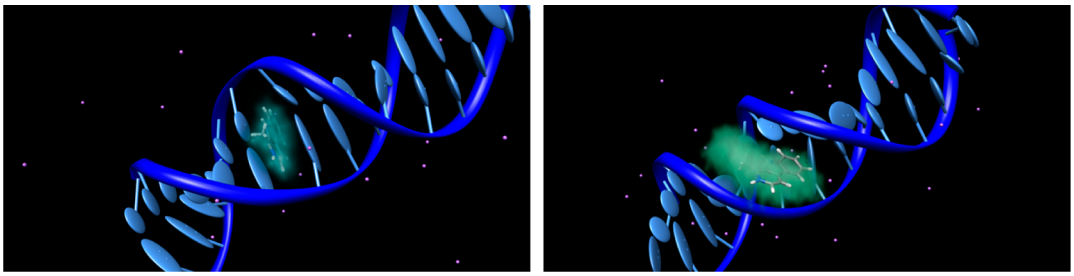

Figure 6. Representative figures of Har^+ interacting with DNA; left, intercalation mode; right, minor groove-binding. The green halo represents the region of space spanned by Har^+ during the simulation. DNA is represented in cartoon.

along the groove itself. Note also that the intercalation induces an important deformation of DNA basis: the distance between the two base pairs in direct contact with the intercalator needs to augment considerably to accommodate the molecule, and it is practically doubled compared to the unperturbed DNA structure. In any case, for the two conformations, the global double helix B-structure of the macromolecule is preserved.

The stability of the two interaction modes is also confirmed from the potential energy plot reported in Figure 7.

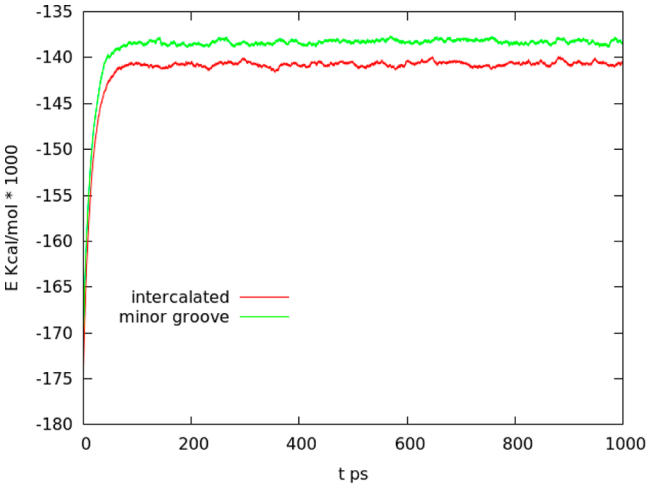

Figure 7. Potential energy for the Har^+ cation interacting with DNA; results extracted from MD trajectory.

One can see that after thermalization both interaction modes reach a quite stable plateau experiencing no significant deviation or discontinuity that could be the signature of the passage from one stable conformation to another one. Note also that apparently the intercalation mode appears to have lower potential energy than minor groove binding, even though the small energy difference would suggest that both modes could coexist.

In Figure 8 we report the TD-DFT spectra computed at QM/MM level convoluted from different snapshots of the previous trajectory. Note that only the wavelengths larger than 300 nm have been reported to exclude the part of the spectrum dominated by DNA absorption. Once again one can notice a very good agreement with experimental results characterized by an absorption band centered at 370 nm and a very intense band appearing at around 300 nm. Note that the intercalation mode absorption maximum appears closer to the experimental result than the one of the groove-binding structure, the latter giving absorption at about 380 nm. This is anyway still largely inside the error limit of the method. Apart from the absorption maximum, it has to be underlined that TDDFT, combined with MD, gives quite a more asymmetric absorption band showing a larger tail toward the red regions of the spectrum. The general band-shape fits very well the observed absorption band of Har^+ in DNA aqueous solutions.[20]

Note also that the same tendencies underlined in the case of water solution are also presented. In particular, pure mechanical effects (ME) give a much red-shifted spectrum, generating a very large band centered at about 400 nm for both intercalation

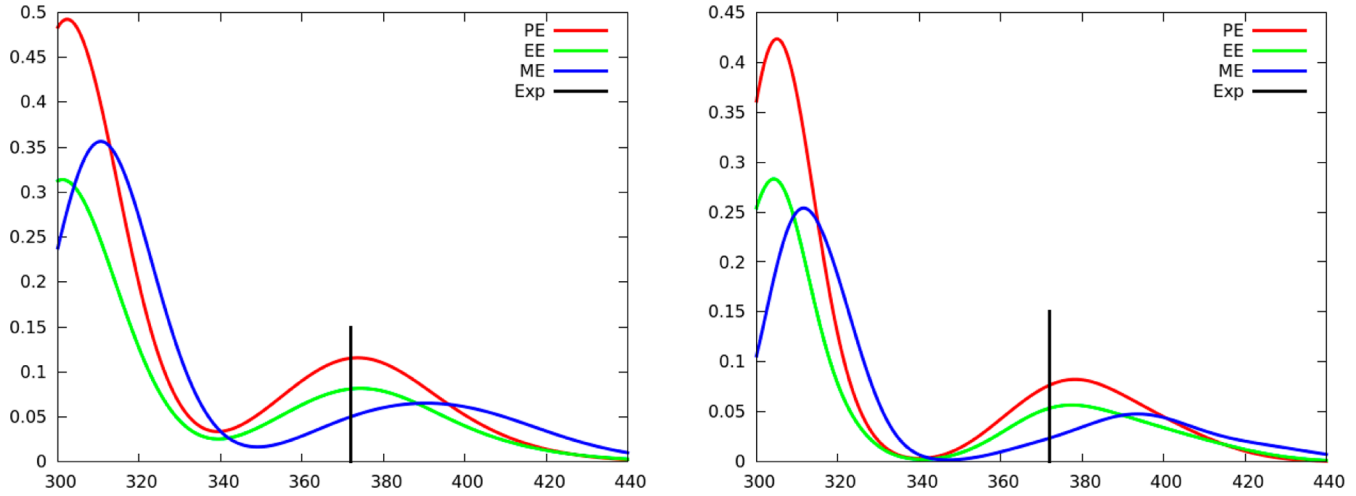

Figure 8. TD-DFT for the Har^+ interacting with DNA. Intercalation on the left and minor groove binding on the right. Wavelengths in nanometers; intensities in arbitrary units.

dx.doi.org/10.1021/jp4017882 | J. Phys. Chem. B XXXX, XXX, XXX−XXX

modes. Electrostatic effects (EE) once again shift the absorption maximum toward the blue, but apparently less efficiently for groove-binding than for intercalation mode. Finally, polarization (PE) again slightly and partially compensates the blue-shift in the case of both interaction modes. Notice, in particular that even when in interaction with the DNA, both by minor groove-binding and by intercalation, the chromophore molecule still experiences the vibrational motion leading to the loss of the planarity of the conjugated system and hence to a significant red-shifted absorption.

CONCLUSIONS

We have reported the theoretical study of the absorption spectrum of a β-carboline, harmane, in different environments. In particular, we have considered aqueous solutions and interaction with DNA. It appears evident that the treatment of the environment is crucial in such a system and will strongly influence the quality of the obtained spectra. Particular care should be taken in considering the subtle interplay between vibrational degrees of freedom of the chromophore and the different environment (solvent) conformations. Indeed, it clearly appears that the usual and less time-consuming procedure to model absorption spectra, i.e., performing a calculation from equilibrium geometry, is totally unreliable for such a system. Note anyway that the shift in absorption wavelength is due to dynamic (vibrational) effects rather than electronic ones. Indeed, the drawback of the conventional static approach is not due to a deficiency of the PCM model in reproducing the electronic solvent effects.

The static approach gives a blue shift of the absorption maximum of about 40−50 nm; paradoxically gas phase calculation gives much better agreement with experience, due to error cancellation. The inclusion of solvent effects by means of an MD trajectory, which also allows one to take into account the vibrational motion of the chromophores, and subsequent QM/MM calculations on selected snapshots are able to retrieve the correct behavior of the spectrum. Indeed, geometric and vibrational effects induce a distortion of the planarity of the molecules that breaks the conjugation of the three-ring system, destabilizing the ground state, and hence red-shifting the absorption. Electrostatic and polarization effects, on the other hand, diminish the latter destabilization effects. It also appears evident that to get a clear picture of both intensities and absorption maxima, electrostatic effects should be taken into account together with the polarization of the environment.

As far as the interaction between DNA and the harmane cation is concerned, we have clearly shown, again by means of MD technique, the existence of two stable interaction modes: intercalation and groove-binding through the minor groove. Both interaction modes give rise to similar absorption spectra. The overall similarity of the absorption spectra for the two interaction modes, with a difference of only 10 nm in absorption maxima, makes it impossible to discriminate between intercalation and groove-binding, especially since the MD trajectory suggests that both modes lead to stable aggregates between Har^+ and DNA.

In the future we plan to extend the present work to take into account the emission properties of the Har^+ cation. Particular attention will be devoted to the necessity to clearly follow the geometric reorganization in the excited state upon vertical excitation, as well as to properly take into account the reorganization and relaxation of the environment, solvent or macromolecular structure, which can strongly affect the shape and position of the fluorescence spectrum.

AUTHOR INFORMATION

Corresponding Author

*E-mail: antonio.monari@univ-lorraine.fr.

Notes

The authors declare no competing financial interest.

ACKNOWLEDGMENTS

Support from the University of Lorraine is acknowledged. A.M. thanks CNRS for the funding of the “Chaire d’excellence” program. ANR Blanc PhotoBioMet is also gratefully acknowledged.

REFERENCES

(1) Very, T.; Despax, S.; Hébraud, P.; Monari, A.; Assfeld, X. *Phys. Chem. Chem. Phys.* **2012**, *14*, 12496−12504.
(2) Chantzis, A.; Very, T.; Monari, A.; Assfeld, X.. *J. Chem. Theory Comput.* **2012**, *8*, 1536−1541.
(3) Metclafe, C.; Thomas, J. A. *Chem. Soc. Rev.* **2003**, *32*, 215−224.
(4) Ortmans, I.; Elias, B.; Kelly, J. M.; Moucheron, C.; Kirsch-De Mesmaeker, A. *Dalton Trans.* **2004**, 668−676.
(5) Jin-Gang, L.; Bao-Hui, Y.; Hong, L.; Liang-Nian, J.; Jian-Ying, Z. J. *Inorg. Biochem.* **1999**, *73*, 117−123.
(6) Matson, M.; Svensson, F. R.; Nordén, B.; Lincoln, P. *J. Phys. Chem. B* **2011**, *115*, 1706−1711.
(7) Kobayashi, H.; Ogawa, M.; Alford, R.; Choyke, P. L.; Urano, Y. *Chem. Rev.* **2011**, *110*, 2620−2640.
(8) Herman, S.; Ghosh, S.; Defrancq, E.; Kirsch-De Mesmaeker, A. *J. Phys. Org. Chem.* **2008**, *21*, 670−681.
(9) Levina, A.; Mitra, A.; Lay, P. A. *Metallomics* **2009**, *1*, 458−470.
(10) Gill, M. R.; Thomas, J. A. *Chem. Soc. Rev.* **2012**, *41*, 3179−3192.
(11) Hartingera, C. G.; Zorbas-Seifriedb, S.; Jakupeca, M. A.; Kynastc, B.; Zorbasb, H.; Keppler, B. K. *J. Inorg. Chem.* **2006**, *100*, 891−904.
(12) Rosenberg, B.; Vamcamp, L.; Trosko, J. E.; Mansour, V. H. *Nature* **1969**, *222*, 385−386.
(13) Cerón-Carrasco, J. P.; Jacquemin, D.; Cauët, E. *Phys. Chem. Chem. Phys.* **2012**, *14*, 12457−12464.
(14) Satoh, M.; Naganuma, A.; Imura, N. *Cancer Chemother. Pharmacol.* **1988**, *21*, 176−178.
(15) Rajeswaran, A.; Trojan, A.; Burnand, B.; Gianelli, M. *Lung Cancer* **2008**, *59*, 1−11.
(16) Molina, A.; Vaquero, J. J.; Garcia-Navio, J. L.; Alvarez-Builla, J.; de Pascual-Teresa, B.; Gago, F.; Rodrigo, M. M. *J. Org. Chem.* **1999**, *64*, 3907−3915.
(17) Richards, A. D.; Rodger, A. *Chem. Society Rev.* **2007**, *36*, 471−483.
(18) Leczkowska, A.; Vilar, R. *Annual Rep. Section A* **2012**, *108*, 330−349.
(19) Zeglis, B. M.; Pierre, V. C.; Barton, J. K. *Chem. Commun.* **2007**, *44*, 4465−4479.
(20) Paul, B. K.; Guchhait, N. *J. Phys. Chem. B* **2011**, *115*, 11938−11949.
(21) Abtouche, S.; Very, T.; Monari, A.; Brahimi, M.; Assfeld, X. *J. Mol. Model.* **2013**, *19*, 581−588.
(22) Loos, P. F.; Preat, J.; Laurent, A. D.; Michaux, C.; Jacquemin, D.; Perpète, E. A.; Assfeld, X. *J. Chem. Theory Comput.* **2008**, *4*, 637−645.
(23) Laurent, A. D.; Assfeld, X. *Interdiscip. Sci.: Comput. Life Sci.* **2010**, *2*, 38−47.
(24) Friedman, A. E.; Chambron, J.-c.; Sauvage, J.-P.; Turro, N. J.; Barton, J. K. *J. Am. Chem. Soc.* **1990**, *112*, 4960−4962.
(25) Jenkins, Y.; Friedman, A. E.; Turro, N. J.; Barton, J. K. *Biochemistry* **1992**, *31*, 10809−10816.

(26) McKinley, A. W.; Lincoln, P.; Tuite, E. M. *Coord. Chem. Rev.* **2011**, *255*, 2676−2692.
(27) Garcia-Zubiri, I. X.; Burrows, H. D.; Seixas de Melo, J. S.; Pina, J.; Monteserin, M.; Tapia, M. J. *Photochem. Photobiol.* **2007**, *83*, 1455−1464.
(28) Elias, B.; Genereux, J. C.; Barton, J. K. *Angew. Chem., Int. Ed.* **2008**, *47*, 9067−9070.
(29) Mondéjar, V. P.; Cuesta, I. G.; Lazzeretti, P.; Sanchez-Marin, J.; de Meras, A. S. *Chem. Phys. Chem.* **2008**, *9*, 896−901.
(30) Jana, B.; Senapati, S.; Ghosh, D.; Bose, D.; Chattopadhyay, N. *J. Phys. Chem. B* **2012**, *116*, 639−645.
(31) Chen, Z.; Cao, R.; Yu, L.; Shi, B.; Sun, J.; Guo, L.; Ma, Q.; Yi, W.; Song, X.; Song, H. *Eur. J. Med. Chem.* **2010**, *45*, 4740−4745.
(32) Garcia-Zubiri, I. X.; Burrows, H. D.; Seixas de Melo, J. S.; Pina, J.; Monteserin, M.; Tapia, M. J. *J. Fluoresc.* **2008**, *18*, 961−972.
(33) Bloom, F.; Barchas, J.; Sandler, M.; Usdin, E. *Prog. Clin. Biol. Res.* **1982**, *90*, 428−429.
(34) Braestrup, C.; Nielsen, M.; Olsen, C. E. *Proc. Natl. Acad. Sci. U.S.A.* **1980**, *77*, 2288−2292.
(35) Carlini, E. A. *Pharmacol., Biochem. Behav.* **2003**, *75*, 501−512.
(36) Nafisi, S.; Panahyab, A.; Sadeghi, G. B. *J. Lumin.* **2012**, *132*, 2361−2366.
(37) Cao, R.; Peng, W.; Wang, Z.; Xu, A. *Curr. Med. Chem.* **2007**, *14*, 479−500.
(38) Herraiz, T. *Beta-Carboline Alkaloids in Bioactive Compounds in Foods*; Blackwell Publishing Ltd.: Oxford, 2008.
(39) Rommelspacher, H.; Kauffmann, H.; Cohnitz, C. H.; Coper, H. *Naunyn-Schmiederberg's Arch. Pharmacol.* **1977**, *298*, 83−91.
(40) Teitel, S.; Brossi, A. *Lloydia* **1974**, *37*, 196−211.
(41) Roberts, M. F. ; Wink, M. *Alkaloids Biochemistry, Ecology and Medicinal Applications*; Plenum Press: New-York, 1988.
(42) Arshad, N.; Zitterl-Eglseer, K.; Hasnain, S.; Hess, M. *Phytother. Res.* **2008**, *22*, 1533−1538.
(43) Di Giorgio, C.; Delmas, F.; Ollivier, E.; Elias, R.; Balansard, G.; Timon-David, P. *Exp. Parasitol.* **2004**, *106*, 67−74.
(44) Hudson, J. B.; Towers, G. H. *Pharmacol. Ther.* **1991**, *49*, 81−122.
(45) Hashimoto, Y.; Kawanishi, K.; Morriyasu, M. In *The Alkaloids: Chemistry and Pharmacology*; Brossi, A., Ed.; Academic Press: San Diego, CA, 1988; Vol. *32*, pp 4045.
(46) Kikura-Hanajiri, R.; Hayashi, M.; Saisho, K.; Goda, Y. *J. Chromatogr. B* **2005**, *825*, 29−37.
(47) Cooper, E. J.; Hudson, A. L.; Parker, C. A.; Morgan, N. G. *Eur. J. Pharmacol.* **2003**, *482*, 189−196.
(48) Boursereau, Y.; Coldham, I. *Bioorg. Med. Chem. Lett.* **2004**, *14*, 5841−5844.
(49) Laronze, M.; Boisbrun, M.; Léonce, S.; Pfeiffer, B.; Renard, P.; Lozach, O.; Meijer, L.; Lansiaux, A.; Bailly, C.; Sapi, J.; Laronze, J.-Y. *Bioorg. Med. Chem.* **2005**, *13*, 2263−2283.
(50) Tu, L. C.; Chen, C.-S.; Hsiao, I.-C.; Chern, J.-W.; Lin, C.-H.; Shen, Y.-C.; Yeh, S. F. *Chem. Biol.* **2005**, *13*, 2263−2283.
(51) Cao, R.; Peng, W.; Chen, H.; Ma, Y.; Liu, X.; Hou, X.; Guan, H.; Xu, A. *Biochem. Biophys. Res. Commun.* **2005**, *338*, 1557−1563.
(52) Gonzalez, M. M.; Arnbjerg, J.; Denofrio, M. P.; Erra-Balsells, R.; Ogilby, P. R.; Cabrerizo, F. M. *J. Phys. Chem. A* **2009**, *113*, 6648−6656.
(53) Shin, H. J.; Lee, H. S.; Lee, D. S. *J. Microbiol. Biotechnol.* **2010**, *20*, 501−505.
(54) Dolmans, D.E.J.G.J.; Fukumura, D.; Jain, R. K. *Nat. Rev. Cancer* **2003**, *3*, 380−387.
(55) Allison, R. R.; Downie, G. H.; Cuenca, R.; Hu, X.-H.; Childs, C. J. H.; Sibata, C. H. *Photodiagn. Photodyn. Ther.* **2004**, *1*, 27−42.
(56) Jacquemin, D.; Perpète, E. A.; Laurent, A. D.; Assfeld, X.; Adamo, C. *Phys. Chem. Chem. Phys.* **2009**, *11*, 1258−1262.
(57) Laurent, A. D.; Assfeld, X. *Interdiscip. Sci.: Comput. Life Sci.* **2010**, *2*, 38−47.
(58) Tomasi, J.; Menucci, B.; Cammi, R. *Chem. Rev.* **2005**, *105*, 2999−3093.
(59) Assfeld, X.; Monari, A.; Rivail, J.-L. *Acc. Chem. Res.* **2012**, DOI: 10.1021/ar300278j.
(60) Gao, J. *Rev. Comput. Chem.* **1996**, *7*, 119−185.
(61) Caprasecca, S.; Curutchet, C.; Menucci, B. *J. Chem. Theory Comput.* **2012**, *8*, 4462−4473.
(62) Monard, G.; Merz, K. M. *Acc. Chem. Res.* **1999**, *32*, 904−911.
(63) Lin, H.; Truhlar, D. G. *Theor. Chem. Acc.* **2007**, *117*, 185−199.
(64) Senn, H. M.; Thiel, W. *Ang. Chem., Int. Ed.* **2009**, *48*, 1198−1229.
(65) Gordon, M. S.; Fedorov, D. G.; Pruitt, S. R.; Slipchenko, L. V. *Chem. Rev.* **2012**, *112*, 632−672.
(66) Cances, E.; Menucci, B.; Tomasi, J. *J. Chem. Phys.* **1997**, *107*, 3032−3041.
(67) Menucci, B.; Cances, E.; Tomasi, J. *J. Phys. Chem. B* **1997**, *101*, 10506−10517.
(68) Clark, T.; Chandrasekhar, J.; Spitznagel, G. W.; Schleyer, P. V. R. *J. Comput. Chem.* **1983**, *4*, 294−301.
(69) Adamo, C.; Barone, V. *J. Chem. Phys.* **1999**, *110*, 6158−6170.
(70) Becke, A. D. *J. Chem. Phys.* **1993**, *98*, 5648−5652.
(71) Yanai, T.; Tex, D. P.; Handy, N. C. *Chem. Phys. Lett.* **2004**, *393*, 51−57.
(72) Jorgensen, W. L.; Chandrasekhar, J.; Madura, J. D.; Impey, R. W.; Klein, M. L. *J. Chem. Phys.* **1983**, *79*, 926−935.
(73) Wang, J.; Wolf, R. M.; Caldwell, J. W.; Kollman, P. A. *J. Comput. Chem.* **2004**, *25*, 1157−1174.
(74) Rick, S. W.; Stuart, S. J. *Rev. Comp. Chem.* **2002**, *18*, 89−146.
(75) Garrec, J.; Patel, C.; Rothlisberger, U.; Dumont, E. *J. Am. Chem. Soc.* **2012**, *134*, 2111−2119.
(76) Cornell, W. D.; Cieplak, P.; Bayly, Bayly, C. I.; Gould, I. R.; Merz, K. M.; Ferguson, D. M.; Spellmeyer, D. C.; Fox, T.; Calwell, J. W.; Kollman, P.A. J. *Am. Chem. Soc.* **2002**, *117*, 5179−5197.
(77) Frisch, M. J. ; Trucks, J. W. ; Schlegel, H. B. et al.. *Gaussian 09*, revision B.01; Gaussian, Inc.: Wallingford, CT, 2009.
(78) TINKER Molecular Modeling Software. http://dasher.wustl.edu/ffe/Tinker.
(79) (a) Angeli, C.; Cimiraglia, R.; Evangelisti, S.; Leininger, T.; Malrieu, J.-P. *J. Chem. Phys.* **2001**, *114*, 10252. (b) Angeli, C.; Cimiraglia, R.; Malrieu, J.-P. *Chem. Phys. Lett.* **2001**, *350*, 297−305. (c) Angeli, C.; Cimiraglia, R.; Malrieu, J.-P. *J. Chem. Phys.* **2002**, *117*, 9138.
(80) Neese, F. *Wiley Interdiscip. Rev.: Comput. Mol. Sci.* **2012**, *2*, 73−78.
(81) Phillips, J. C.; Braun, R.; Wang, W.; Gumbart, J.; Tajkhorshid, E.; Villa, E.; Chipot, C.; D. Skeel, R.; Kale, L.; Schulten, K. *J. Comput. Chem.* **2005**, *26*, 1781−1802.
(82) Jacquemin, D.; Mennucci, B.; Adamo, C. *Phys. Chem. Chem. Phys.* **2011**, *13*, 16987−16989.